



# Rational Approximation of Unsteady Friction Weighting Functions in the Laplace Domain

Robin Julian<sup>1</sup>; Didier Dragna<sup>2</sup>; Sébastien Ollivier<sup>3</sup>; and Philippe Blanc-Benon<sup>4</sup>

**Abstract:** This paper aims at improving the weighting function based-method (WFB) for modeling the transient behavior of a laminar flow in cylindrical pipes in a one-dimensional approach. Two improvements for the numerical computation of the unsteady friction term are presented. First, a rational approximation of the weighting function in the Laplace domain is preferred instead of an exponential series fit in the time domain. It allows the WFB method to be improved in terms of validity for small time steps, accuracy, and computational efficiency. Second, the use of auxiliary differential equations to compute convolution makes the high order time-integration of the frequency-dependent friction term straightforward, without the assumption of a constant acceleration during the time step. The simulation results for a well-known experimental test case show a good agreement of the derived methods with the experiment. Finally, the time stability of the discretized problem is fully analyzed, and a stability condition for the WFB method is brought out. DOI: [10.1061/\(ASCE\)HY.1943-7900.0001905](https://doi.org/10.1061/(ASCE)HY.1943-7900.0001905). © 2021 American Society of Civil Engineers.

## Introduction

When the equation of fluid motion is applied in a one-dimensional (1D) approach, all components of viscous diffusion terms vanish, and this leads to a lossless model. To overcome this major issue, the effects of viscosity are classically taken into account as an external effort derived from the wall shear stress. Viscosity effects are then embedded in the friction term. In the case of a steady laminar pipe flow (i.e., with a parabolic velocity profile), the use of the analytical Hagen-Poiseuille law results in proportionality between the friction and the mean flow velocity. This law is frequently extended to unsteady flow by means of a quasi-steady approximation. However, the rapid evolution of the velocity profile is inconsistent with a parabolic one, and the resulting decay of the pressure wave is underestimated. Thus, viscosity effects occurring in the radial dimension have to be represented differently in the 1D friction term.

Holmboe and Rouleau (1967) pioneered the need for a frequency-dependent friction term to explain the fast decay of the pressure

histories during water hammer phenomena. Since then, the three approaches listed subsequently have been developed to account for unsteady friction with efficient numerical computation:

- The weighting function-based (WFB) method, in which the unsteady contribution of the friction is defined by a convolution of the past acceleration and the so-called weighting function (Zielke 1968);
- The quasi-two-dimensional (quasi 2D) method, in which the transverse component of velocity is modeled by the method of characteristics applied in concentric cylindrical annuli (Vardy and Hwang 1991); and
- The instantaneous acceleration-based (IAB) method, in which the unsteady wall shear stress is in relationship with the local instantaneous acceleration (Brunone et al. 1995, 2004).

For the laminar pipe flow, the WFB method is popular because it offers the best trade-off between accuracy and computational cost, provided the weighting function [analytically found by Zielke (1968)] is written as an exponential series. Indeed, such a formulation allows numerical integration to be implemented in recursive formulas that are well suited for time-marching methods like methods of characteristics or Runge-Kutta algorithms (Triakha 1975; Suzuki et al. 1991).

The problem of the fitting exponential sum is difficult mainly due to the nonuniqueness of the solution. Consequently, results are very method-dependent. A series of papers (Triakha 1975; Kagawa et al. 1983; Schohl 1993; Taylor et al. 1997; Vardy and Brown 2004; Vítkovský et al. 2004; Jiang et al. 2015; Urbanowicz 2018) present various methods in order to find the coefficients of the exponential series in the time domain. These can be classified into three categories: knots-based method, least squared relative error minimization method, and genetic algorithm-based method. Despite the great improvements made, there are still some practical cases in which the required time step is so small that the approximate function is no longer valid or may cause numerical instabilities.

The main purpose of this paper is to give an alternative method for the approximation of the Zielke (1968) weighting function into an exponential series based on a rational approximation in the Laplace domain. The new method aims to a better trade-off between the validity and the accuracy of the approximated weighting function. The authors' motivation is to extend the WFB method to flow

<sup>1</sup>Doctor, Zone d'Aménagement Concerté du Baconnet, EFS Sa, 192 Allée des Chênes, Montagny F-69700, France (corresponding author). Email: [rjulian@efs.fr](mailto:rjulian@efs.fr)

<sup>2</sup>Assistant Professor, Ecole Centrale de Lyon, Institut National des Sciences Appliquées Lyon, Université Claude Bernard Lyon I, Centre National de Recherche Scientifique, Laboratoire de Mécanique des Fluides et d'Acoustique Unité Mixte de Recherche 5509, Université de Lyon, 36 Ave. Guy de Collongue, Écully F-69134, France. ORCID: <https://orcid.org/0000-0002-7497-9130>

<sup>3</sup>Assistant Professor, Ecole Centrale de Lyon, Institut National des Sciences Appliquées Lyon, Université Claude Bernard Lyon I, Centre National de Recherche Scientifique, Laboratoire de Mécanique des Fluides et d'Acoustique Unité Mixte de Recherche 5509, Université de Lyon, 36 Ave. Guy de Collongue, Écully F-69134, France.

<sup>4</sup>Senior Researcher, Ecole Centrale de Lyon, Institut National des Sciences Appliquées Lyon, Université Claude Bernard Lyon I, Centre National de Recherche Scientifique, Laboratoire de Mécanique des Fluides et d'Acoustique Unité Mixte de Recherche 5509, Université de Lyon, 36 Ave. Guy de Collongue, Écully F-69134, France.

Note. This manuscript was submitted on July 21, 2020; approved on March 18, 2021; published online on July 6, 2021. Discussion period open until December 6, 2021; separate discussions must be submitted for individual papers. This paper is part of the *Journal of Hydraulic Engineering*, © ASCE, ISSN 0733-9429.

simulation cases in which either the required time step is small, the pipe diameter large, or the fluid viscosity low. Additionally, several improvements on the numerical computation of viscous friction terms are detailed. Particularly, the use of the auxiliary differential equation (ADE) method combined with the finite-difference time-domain (FDTD) method no longer requires the assumption of a constant acceleration between two consecutive time steps.

The first part of the present paper brings up the problem of the water hammer leading to the fast hydraulic transients in pipes. A 1D model consisting of basic equations together with the WFB method is detailed. The new methods for the weighting function approximation and the numerical computation are then presented. The second part gives the results of the approximate weighting functions and a simulation of a known experimental test case. Limitations of the new methods and further works are finally discussed.

## Method

### Basic Equations

Slightly compressible unsteady pipe flows are governed by the mass and momentum linearized equations, respectively given in a 1D approach by Chaudhry (2014)

$$\frac{\partial H}{\partial t} + \frac{a^2}{g} \frac{\partial V}{\partial x} = 0 \quad (1)$$

$$\frac{\partial H}{\partial x} + \frac{1}{g} \frac{\partial V}{\partial t} + h_s + h_u = 0 \quad (2)$$

where  $H$  = piezometric head;  $V$  = mean sectional velocity;  $g$  = gravitational acceleration;  $a$  = wave speed;  $t$  = time;  $x$  = distance;  $h_s$  = quasi-steady friction term; and  $h_u$  = unsteady friction term. The two dimensionless friction terms are derived from the wall shear stress,  $\tau_0$

$$h_s + h_u = \frac{2\tau_0}{\rho g R} \quad (3)$$

where  $\rho$  = fluid density.

Consider a hydraulic system with a horizontal cylindrical pipe of length  $L$  and radius  $R$ . The pipe is equipped with a valve and is connected to two upstream and downstream tanks, as shown in Fig. 1.

The two tanks are filled with constant heads  $H_{01} > H_{02}$ , such that the initial flow velocity,  $V_0$ , is sufficiently small to keep the flow laminar. At the initial time,  $t = t_0$ , the valve is closed instantaneously, and this triggers the water hammer phenomenon. Theoretical head and velocity histories for  $t > t_0$  can be obtained on the fluid domain depicted in Fig. 1 by solving the two hyperbolic nonlinear partial differential equations [Eqs. (1) and (2)] with a numerical method (see the section ‘‘FDTD Method’’).

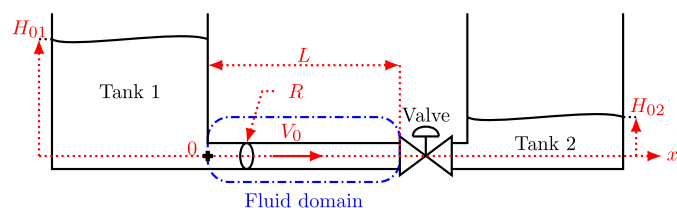


Fig. 1. Tank-pipe-valve-tank system.

### WFB Method

When solving the equation of motion for parallel axisymmetric flow (i.e., in 2D) of an incompressible fluid in the Laplace domain, Zielke (1968) found the following equations between the mean sectional velocity  $V$  and the unsteady wall shear stress  $\tau_0$

$$\hat{\tau}_0(s) = \hat{\Phi}(s) \frac{\partial \hat{V}}{\partial t}(s) \quad (4)$$

$$\hat{\Phi}(s) = \frac{\rho R}{\mathcal{J}_1(j\sqrt{s}\nu R) - 2} \quad (5)$$

where  $\hat{\tau}_0$  = Laplace transform of  $\tau_0$ ;  $\nu$  = kinematic viscosity of the fluid;  $s$  = complex frequency;  $J$  = complex number; and  $\mathcal{J}_i(s) = sJ_{i-1}(s)/J_i(s)$  is the  $i$ th modified quotient of Bessel functions of the first kind and of order  $(i-1)$ th and  $i$ th, respectively. The inverse Laplace transformation of Eq. (5) performed by Zielke (1968) leads to the following result for the steady friction term

$$h_s = \frac{8}{\theta g} V \quad (6)$$

where  $\theta = R^2/\nu$  is the characteristic time of viscosity. Eq. (6) is consistent with the Darcy-Weisbach formula combined with the Hagen-Poiseuille law. Because the wall shear stress is expressed as a product of two functions in the Laplace domain, then the unsteady friction term is a convolution in the time domain

$$h_u = \frac{4}{\theta g} \int_0^t \frac{\partial V}{\partial t} W(t-u) du \quad (7)$$

where  $W$  = weighting function piecewise defined by Zielke (1968) as a function of the dimensionless time,  $\tau = t/\theta$  as follows

$$W(\tau) = \begin{cases} \sum_{i=1}^6 \alpha_i \tau^{(i-2)/2} & \text{for } \tau < 0.02 \\ \sum_{i=1}^5 \exp(-\beta_i \tau) & \text{for } \tau \geq 0.02 \end{cases} \quad (8)$$

where  $\alpha_i$  and  $\beta_i$  are the components of the vectors  $[0.282095 - 1.251.0578550.93750.396696 - 0.351563]^T$  and  $[26.374470.8493135.0198218.9216322.5544]^T$ , respectively.

Direct numerical computation of Eq. (7) is very resource-demanding in terms of memory because the past acceleration needs to be stored for each node. This limits most of the current applications to such an extent that the 1D approach no longer takes benefit from computational cost advantages compared to a 2D approach. Fortunately, the recursive methods developed by Trikha (1975) and Suzuki et al. (1991) decrease the required computer storage to a lower level. The weighting function in Eq. (8) requires it to be approximated by an exponential series of  $N$  pairs of coefficients  $(m_i, n_i) \in \mathbb{R}^2$  as follows

$$W(\tau) \approx W_{\text{app}}(\tau) = \sum_{i=1}^N m_i \exp(-n_i \tau) \quad (9)$$

Methods employed to fit  $W_{\text{app}}$  to  $W$  can be classified in three categories: knots-based (Trikha 1975; Kagawa et al. 1983; Vardy and Brown 2004), least squared relative error minimization (Schohl 1993; Vítkovský et al. 2004), and genetic algorithm-based (Taylor et al. 1997; Jiang et al. 2015). The present paper suggests a new alternative computational method (see the section ‘‘ADE Method’’).

**Table 1.** Coefficients  $m_i$  of the new approximation  $W_{app}$ 

| $N$      | 3                   | 4                   | 5                   | 6                   | 7                   | 8                   | 9                   | 10                  |
|----------|---------------------|---------------------|---------------------|---------------------|---------------------|---------------------|---------------------|---------------------|
| $m_1$    | 1.8056              | 1.4576              | 1.2800              | 1.1786              | 1.1168              | 1.0778              | 1.0526              | 1.0360              |
| $m_2$    | 8.0225              | 4.6663              | 3.3301              | 2.6247              | 2.1933              | 1.9051              | 1.7013              | 1.5516              |
| $m_3$    | $7.2419 \cdot 10^1$ | $1.9403 \cdot 10^1$ | $1.0325 \cdot 10^1$ | 6.9132              | 5.1888              | 4.1674              | 3.4994              | 3.0320              |
| $m_4$    | —                   | $1.7153 \cdot 10^2$ | $4.1958 \cdot 10^1$ | $2.0888 \cdot 10^1$ | $1.3290 \cdot 10^1$ | 9.5820              | 7.4507              | 6.0929              |
| $m_5$    | —                   | —                   | $3.6741 \cdot 10^2$ | $8.4122 \cdot 10^1$ | $3.9789 \cdot 10^1$ | $2.4305 \cdot 10^1$ | $1.6952 \cdot 10^1$ | $1.2826 \cdot 10^1$ |
| $m_6$    | —                   | —                   | —                   | $7.3256 \cdot 10^2$ | $1.5946 \cdot 10^2$ | $7.2434 \cdot 10^1$ | $4.2816 \cdot 10^1$ | $2.9063 \cdot 10^1$ |
| $m_7$    | —                   | —                   | —                   | —                   | $1.3839 \cdot 10^3$ | $2.8947 \cdot 10^2$ | $1.2729 \cdot 10^2$ | $7.3253 \cdot 10^1$ |
| $m_8$    | —                   | —                   | —                   | —                   | —                   | $2.5070 \cdot 10^3$ | $5.0791 \cdot 10^2$ | $2.1755 \cdot 10^2$ |
| $m_9$    | —                   | —                   | —                   | —                   | —                   | —                   | $4.3940 \cdot 10^3$ | $8.6768 \cdot 10^2$ |
| $m_{10}$ | —                   | —                   | —                   | —                   | —                   | —                   | —                   | $7.5039 \cdot 10^3$ |

**Table 2.** Coefficients  $n_i$  of the new approximation  $W_{app}$ 

| $N$      | 3                   | 4                   | 5                   | 6                   | 7                   | 8                   | 9                   | 10                  |
|----------|---------------------|---------------------|---------------------|---------------------|---------------------|---------------------|---------------------|---------------------|
| $n_1$    | $3.4107 \cdot 10^1$ | $3.0516 \cdot 10^1$ | $2.8771 \cdot 10^1$ | $2.7826 \cdot 10^1$ | $2.7280 \cdot 10^1$ | $2.6953 \cdot 10^1$ | $2.6751 \cdot 10^1$ | $2.6624 \cdot 10^1$ |
| $n_2$    | $3.5159 \cdot 10^2$ | $2.0157 \cdot 10^2$ | $1.4677 \cdot 10^2$ | $1.1988 \cdot 10^2$ | $1.0448 \cdot 10^2$ | $9.4817 \cdot 10^1$ | $8.8387 \cdot 10^1$ | $8.3934 \cdot 10^1$ |
| $n_3$    | $9.8148 \cdot 10^3$ | $2.0897 \cdot 10^3$ | $9.8343 \cdot 10^2$ | $6.1791 \cdot 10^2$ | $4.4947 \cdot 10^2$ | $3.5657 \cdot 10^2$ | $2.9930 \cdot 10^2$ | $2.6127 \cdot 10^2$ |
| $n_4$    | —                   | $5.6086 \cdot 10^4$ | $9.9645 \cdot 10^3$ | $4.0905 \cdot 10^3$ | $2.3090 \cdot 10^3$ | $1.5399 \cdot 10^3$ | $1.1366 \cdot 10^3$ | $8.9759 \cdot 10^2$ |
| $n_5$    | —                   | —                   | $2.6023 \cdot 10^5$ | $4.0632 \cdot 10^4$ | $1.5056 \cdot 10^4$ | $7.8230 \cdot 10^3$ | $4.8719 \cdot 10^3$ | $3.3949 \cdot 10^3$ |
| $n_6$    | —                   | —                   | —                   | $1.0420 \cdot 10^6$ | $1.4745 \cdot 10^5$ | $5.0422 \cdot 10^4$ | $2.4520 \cdot 10^4$ | $1.4446 \cdot 10^4$ |
| $n_7$    | —                   | —                   | —                   | —                   | $3.7358 \cdot 10^6$ | $4.8906 \cdot 10^5$ | $1.5679 \cdot 10^5$ | $7.2242 \cdot 10^4$ |
| $n_8$    | —                   | —                   | —                   | —                   | —                   | $1.2295 \cdot 10^7$ | $1.5116 \cdot 10^6$ | $4.5973 \cdot 10^5$ |
| $n_9$    | —                   | —                   | —                   | —                   | —                   | —                   | $3.7831 \cdot 10^7$ | $4.4191 \cdot 10^6$ |
| $n_{10}$ | —                   | —                   | —                   | —                   | —                   | —                   | —                   | $1.1040 \cdot 10^8$ |

### Rational Approximation of Zielke's Function in the Laplace Domain

Reversing Zielke's procedure, one can find the following definition of  $W$  in the Laplace domain from Eqs. (5) and (7)

$$\hat{W}(s) = \frac{R}{2\rho\nu} \hat{\Phi}(s) - \frac{2}{s} \quad (10)$$

The second term on the right-hand side in Eq. (10) is subtracted in order to focus only on the unsteady component of the friction. Let  $s' = \theta s$ , so Eq. (10) becomes

$$\hat{W}(s') = \theta \left[ \frac{1}{2\mathcal{J}_1(\sqrt{js'}) - 4} - \frac{2}{s'} \right] \quad (11)$$

where  $\hat{\Phi}$  has been substituted by its definition given in Eq. (5). On the other hand, the Laplace transform of  $W_{app}$  is given as a function of  $s'$  by the following equation

$$\hat{W}_{app}(s') = \theta \sum_{i=1}^N \frac{m_i}{n_i - s'} \quad (12)$$

Finally, the problem of finding an approximate exponential series in the time domain is equivalent to a system identification in the Laplace domain whose frequency response is  $\hat{W}(s')/\theta$ . This can be performed by using the method developed by Gustavsen and Semylen (1999, 2006), and Deschrijver et al. (2008) for electromagnetic system identification purposes. The resulting numerical values found for  $m_i$  and  $n_i$  are given in Tables 1 and 2.

### Numerical Computation

#### ADE Method

The problem associated with the numerical computation of a convolution is current in aeroacoustics when a frequency-dependent

boundary condition is to be solved in the time domain. The method presented in this section is inspired by this background and takes benefit from a method suitable for high order integration of frequency-dependent terms in the time domain given by Troian et al. (2017). Gathering Eqs. (12) and (7), the approximate unsteady friction model can be written

$$h_u = \frac{4}{\theta g} \sum_{i=1}^N m_i I_i \quad (13)$$

where the auxiliary variables  $I_i$  are given

$$I_i = \int_0^t \frac{\partial V}{\partial t} \exp\left[-\frac{n_i}{\theta}(t-u)\right] du \quad (14)$$

The differentiation of  $I_i$  with respect to time is

$$\frac{\partial I_i}{\partial t} = -\frac{n_i}{\theta} \exp\left(-\frac{n_i}{\theta} t\right) \int_0^t \frac{\partial V}{\partial t} \exp\left(\frac{n_i}{\theta} u\right) du + \frac{\partial V}{\partial t} \quad (15)$$

which leads to the  $N$  auxiliary partial differential equations (ADE) given subsequently

$$\frac{\partial I_i}{\partial t} = -\frac{n_i}{\theta} I_i + \frac{\partial V}{\partial t} \quad (16)$$

Gathering basic equations and the developed model for the unsteady friction term, the system in Fig. 1 is fully modeled by the system of  $N + 2$  equations with unknowns  $H$ ,  $V$ , and  $I_i$

$$\begin{aligned} \frac{\partial H}{\partial t} &= -\frac{a^2}{g} \frac{\partial V}{\partial x} \\ \frac{\partial V}{\partial t} &= -g \frac{\partial H}{\partial x} - \frac{4}{\theta} \left( 2V + \sum_{i=1}^N m_i I_i \right) \\ \frac{\partial I_i}{\partial t} &= -\frac{n_i}{\theta} I_i + \frac{\partial V}{\partial t} \end{aligned} \quad (17)$$

where the last term  $\partial V/\partial t$  on the right-hand side can be substituted by the right-hand side of the second equation in order to recast the system of equations in the form  $\partial \mathbf{y}/\partial t = F(\mathbf{y})$ , with the unknown vector  $\mathbf{y} = [HVI_i]^T$ . With this form, the time integration and the spatial differentiation can be performed separately with any appropriate numerical schemes of the desired order. Although the addition of auxiliary variables to the governing equations has no physical meaning, it allows the unsteady friction term to be computed with the same order as the velocity and the pressure head. Contrarily to the recursive methods given by Trikha (1975) or Urbanowicz (2018), it does not require the acceleration to be assumed constant between two consecutive time steps, which leads to a first-order approximation of the unsteady friction term.

### FDTD Method

Among the previously cited papers, most of the authors make use of the method of characteristics in order to solve Eqs. (1) and (2). This section details another method based on the finite-difference approximation of the partial derivatives with respect to  $x$ . With this aim, the fluid domain requires it to be regularly discretized in a mesh with  $N_x$  elements of dimension  $\Delta x$ . The numerical schemes used subsequently are optimized for the minimization of dispersion and dissipation numerical errors. It is worth noting that the numerical schemes have been designed in order to properly simulate the propagation of acoustic waves whose wavelength,  $\lambda$ , respects the condition  $\lambda > 4.6\Delta x$ , given by Bogey and Bailly (2004).

The partial derivative of  $V$  with respect to  $x$  at the node located at  $x_i = i\Delta x$  can be approximated by the following 4th order centered scheme of the  $2n + 1 = 11$  point stencil

$$\forall i \in [n, N_x - n], \frac{\partial u}{\partial x} \Big|_i \approx \frac{1}{\Delta x} \sum_{k=-n}^n c_k u_{i+k} \quad (18)$$

where the coefficients  $c_k = -c_{-k}$  ( $c_0 = 0$ ) match the FD11p scheme given by Bogey and Bailly (2004). Analogous uncentered schemes for nodes close to the boundaries (i.e.,  $\forall i \in [0, n] \cup [N_x - n, N_x]$ ) are used according to Berland et al. (2007). One drawback of the finite-difference approximation is the possible presence of numerical instabilities due to grid-to-grid oscillations. The adaptive spatial filtering procedure described by Bogey et al. (2009) is then employed in order to remove it.

Once the right-hand side terms of Eq. (17) are approximated by finite differences, time integration is performed by the RK46-L numerical scheme given by Berland et al. (2006). This particular Runge-Kutta algorithm is also optimized in terms of the dispersion error, dissipation error, and storage requirement (Berland et al. 2006). The time-marching procedure described previously will give approximate solutions for  $H$  and  $V$  for each  $t = j\Delta t$  and  $j \in [0, N_t]$ , where  $\Delta t$  is the time step, and  $N_t$  is the number of steps. The time step has to respect the following Courant-Friedrichs-Lewy condition for stability purposes

$$\text{CFL} = a \frac{\Delta t}{\Delta x} \leq \text{CFL}_{\max} \quad (19)$$

where CFL, set to 0.9, is the Courant-Friedrichs-Lewy number; and  $\text{CFL}_{\max}$  is a threshold that depends on both the finite-difference schemes and the time-integration scheme and is usually of the order of unity. Fig. 2 summarizes the numerical procedure for the application of the ADE/FDTD method.

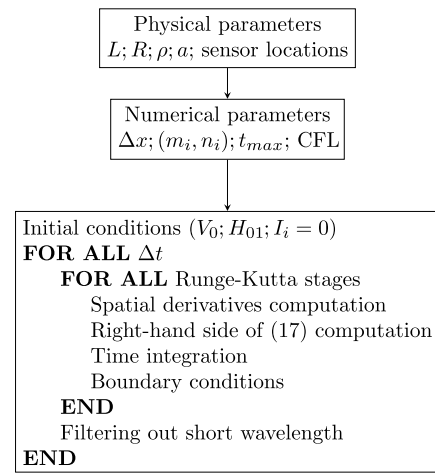


Fig. 2. Flowchart of the numerical algorithm.

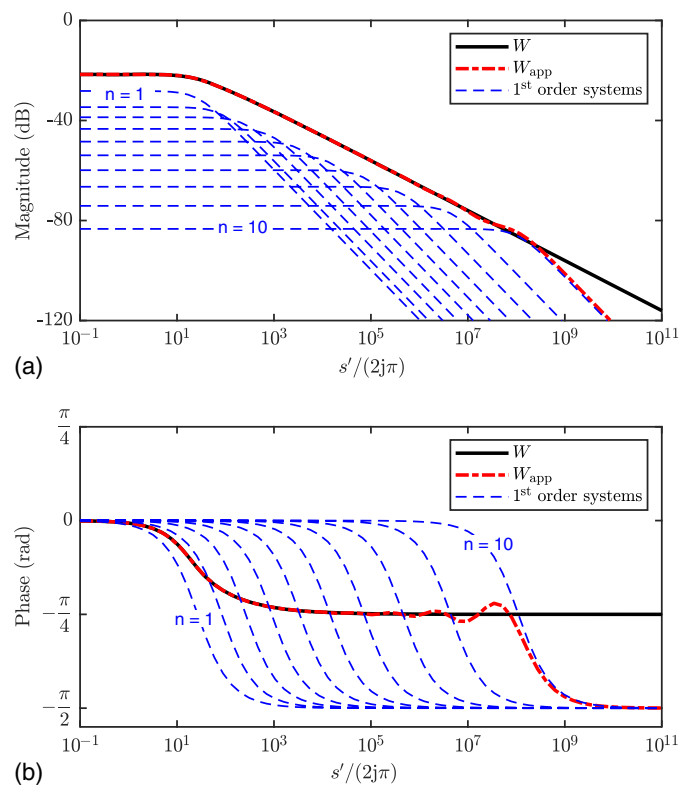


Fig. 3. Bode plot of the exact and the approximative weighting functions of  $N = 10$  terms, with the term's contribution: (a) magnitude; and (b) phase.

## Results

### Approximate Weighting Functions

Let us compare  $W$ ,  $W_{\text{app}}$ , and its  $N = 10$  components with the Bode plot shown in Fig. 3. The magnitude ( $20\log_{10}|W(s')|$ ) and phase are respectively given in decibels and radians, both as a function of the dimensionless frequency  $s'/(2j\pi)$ .

The exact weighting function exhibits a constant value of  $-21.6$  dB from low frequencies to the cutoff frequency near 25 (dimensionless) and drops subsequently with a slope of

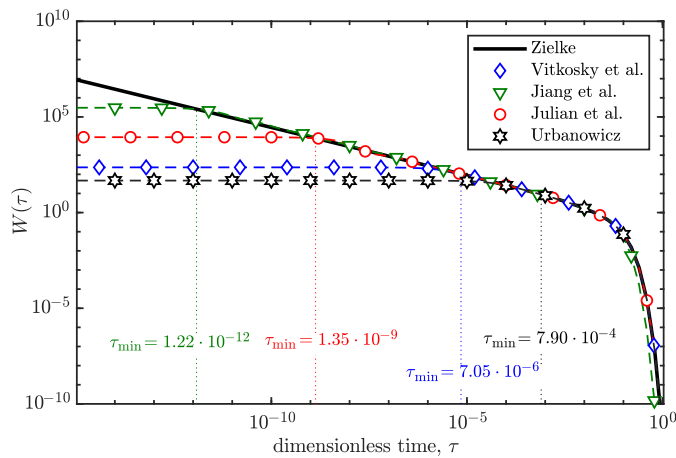


**Fig. 4.** Comparison between the new  $W_{app}$ , the existing  $W_{app}$  of  $N = 10$  terms, and the exact  $W$  in the time domain.

$-10$  dB/decade. The approximative weighting function is made from a sum of first-order systems whose cutoff frequencies equal the  $n_i$  coefficients. Because the frequency response of first-order systems decreases with a slope of  $-20$  dB/decade starting from the cutoff frequency,  $W_{app}$  cannot fit  $W$  properly for frequencies exceeding  $n_N$ . The same observation can be made by looking at the phase mismatch at high frequencies between the components of  $W_{app}$ , whose phases tend to  $-\pi/2$ , and  $W$ , whose phase turns down to  $-\pi/4$ . These phase and magnitude behaviors allow one to find the following equivalence of  $W_{app}$  for high  $s'$

$$W_{app} \underset{s' \rightarrow \infty}{\sim} \frac{m_N}{n_N - s'} \quad (20)$$

Graphically speaking, the  $-10$  dB/decade slope of  $W$  is built from the successive corners of each first-order system frequency response. Consequently, for a given number of terms, there is a trade-off between the accuracy and the validity of the approximation.

Fig. 4 shows a comparison between the weighting function given by Zielke (1968) and the existing approximate 10-term exponential series as a function of the dimensionless time. The function given by Kagawa et al. (1983) has been removed for clarity purposes because its curve is very similar to the one given by Vítkovský et al. (2004).

In the time domain, the weighting function decreases monotonically, with a particularly steep slope for high  $\tau$  (typically  $\tau > 0.04$ ). Bearing in mind the analytical formulation of the unsteady friction term in Eq. (7), it means the more the past acceleration is recent, the stronger it contributes to the viscous dissipation. Starting from a minimum value of dimensionless time  $\tau_{min}$ , the three approximate functions agree well the Zielke's function. For physical consistency of the model, the choice of  $N$  must be in accordance with  $\tau_{min} \leq \Delta t/\theta$  and can be augmented for further accuracy. Considering only this criterion, the function given by Jiang et al. (2015) is the best fit, followed by the new approximate, the function given by Vítkovský et al. (2004) and the one given by Urbanowicz (2018).

In order to find the best trade-off between the accuracy and the validity of the approximation, the validity is assessed with  $\tau_{min}$ , defined as the shortest time when the difference  $W - W_{app}$  changes sign. Alternatively, Vítkovský et al. (2004) and Vardy and Brown (2004) indicate the validity of their own approximations, so the value of  $\tau_{min}$  is taken according to them. The accuracy is assessed using the weighting function approximation error,  $E_W$ , which is numerically computed as in Vítkovský et al. (2006)

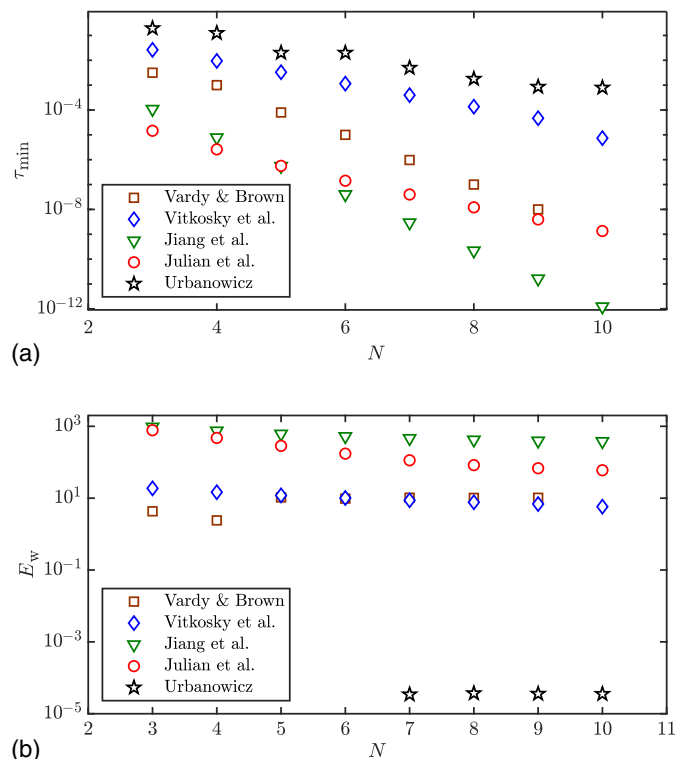


**Fig. 5.** Comparison of the weighting function approximation results depending on the number of terms  $N$ : (a) validity domain; and (b) accuracy.

$$E_W = \sum_{j=M}^P \left[ \frac{W(\tau_j) - W_{app}(\tau_j)}{W(\tau_j)} \right]^2 \quad (21)$$

where the integers  $M$  and  $P$  are such as  $P - M + 1 = 1,000$ . Additionally, the  $\tau_j$  are distributed between  $\tau_M = \tau_{min}$  and  $\tau_P = 1$  with a logarithmic scale. Fig. 5 emphasizes the antagonism between the accuracy and the validity of the approximation methods.

In fact, the method employed by Jiang et al. (2015) achieves a great extend of validity but poor accuracy and conversely for the method of Urbanowicz (2018). Finally, the new method suggested in the present paper gives the best trade-off for  $N \in [5, 9]$ . Outside this interval, the authors recommend the use of the approximation of Vardy and Brown (2004). If very small  $\tau_{min}$  is required, only the approximation of Jiang et al. (2015) can fit because their  $(m_i, n_i)$  coefficients are defined by a geometric series with an unlimited number of terms  $N$ .

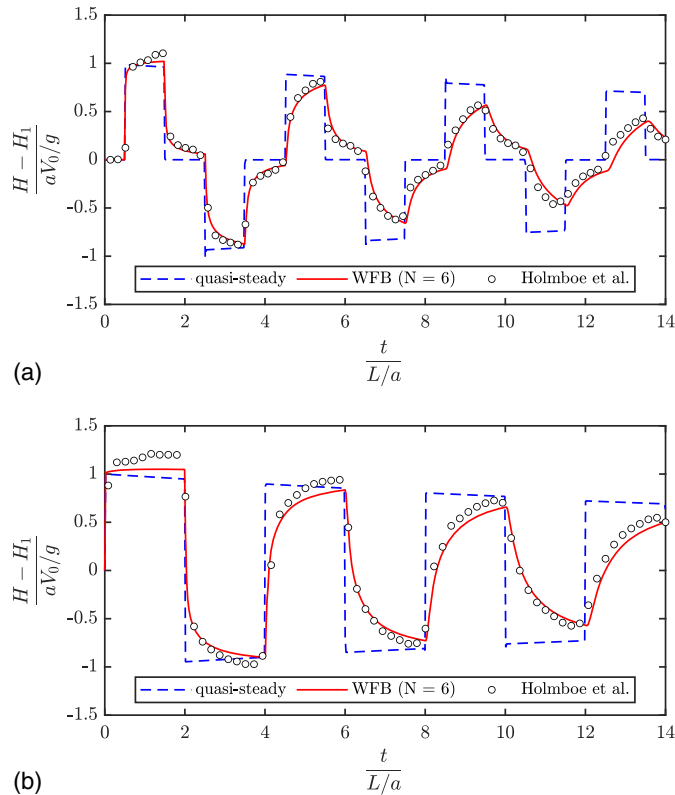
### Simulation Test Case

Let us apply the FDTD with the ADE methods to the problem of the water hammer occurring in the tank-pipe-valve-tank hydraulic system presented in Fig. 1. The initial state is a laminar steady-state flow with  $V(t=0) = V_0$  and  $H(t=0) = H_{01} - 8V_0/(g\theta)x$ . All auxiliary variables are initially null because  $\partial V/\partial t = 0$  [Eq. (14)]. The boundary conditions are constant-level [i.e.,  $H(x=0) = H_{01}$ ] and dead end [i.e.,  $V(x=L) = 0$ ] (Chaudhry 2014). The simulation parameters gathered in Table 3 are taken from the experimental study presented by Holmboe and Rouleau (1967).

Additionally, the duration of the simulation is chosen to allow the wavefront to travel back and forth in the pipe seven times, thus for a rigid pipe  $14 L/a = 0.38$  s. In accordance with Holmboe and Rouleau (1967), the head and the velocity of the flow are recorded

**Table 3.** Simulation parameters

| Parameters                 | Value                                      |
|----------------------------|--|
| Kinematic viscosity: $\nu$ | $39.67 \cdot 10^{-6} \text{ m}^2/\text{s}$ |
| Density: $\rho$            | $998.2 \text{ kg/m}^3$                     |
| Initial velocity: $V_0$    | $0.12 \text{ m/s}$                         |
| Pipe length: $L$           | $36.088 \text{ m}$                         |
| Pipe radius: $R$           | $1.27 \text{ cm}$                          |
| Wave speed: $a$            | $1,324.36 \text{ m/s}$                     |
| Time step: $\Delta t$      | $5.84 \mu\text{s}$                         |

**Fig. 6.** FDTD/ADE simulation results of the water hammer with quasi-steady and WFB approaches. Head histories at (a)  $x = x_1$ ; and (b)  $x = L$ .

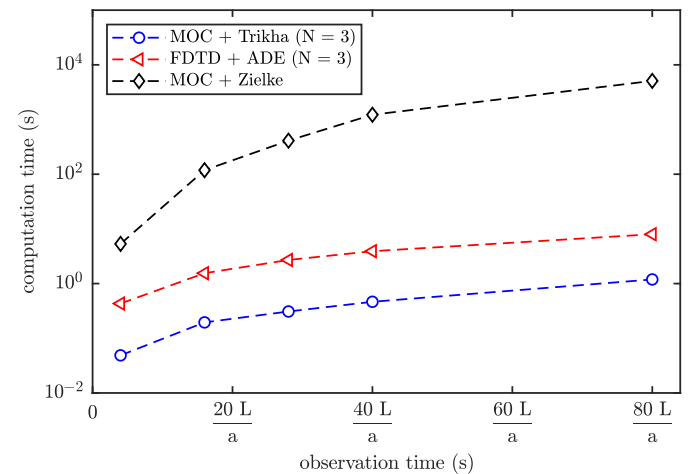
with two pressure sensors, one located at  $x_1 = 17.8 \text{ m}$  and the other at the valve location ( $x_2 = L$ ). The dimensionless head histories at these two locations are shown in Fig. 6.

Simulation results are very close to the experimental results of Holmboe and Rouleau (1967). It is also consistent with the Allievi and Joukovsky equations that predict the wave speed  $a$  and the maximum pressure surge of  $aV_0/g$ , respectively. Nevertheless, one can notice the slight augmentation (approximately 5%) of the maximum pressure surge in the unsteady model and the measurements that are not predicted by the Joukovsky equation. The contribution of the unsteady friction is clearly visible with the filtering of the high-frequency content in the quasi-steady friction model, which produces unlikely steep rising and falling edges in the head histories. As shown in Table 4, the root mean squared deviations (RMSD) between the simulation and the experiment (i.e., including the measurement uncertainties) is near 0.008 for large  $N$ . From a more practical point of view, Fig. 7 allows one to appreciate the benefit of the proposed method in terms of computational efficiency.

**Table 4.** Root mean squared deviation between the simulated and the measured head histories at  $x = x_1$  with an indication of the simulation time for the different models

| $N$ | RMSD                |                        |               |              | Simulation time (s) |
|-----|---------------------|------------------------|---------------|--------------|---------------------|
|     | Jiang et al. (2015) | Vardy and Brown (2004) | Present paper | Quasi-steady |                     |
| 0   | —                   | —                      | —             | 0.0197       | 300                 |
| 2   | 0.0112              | —                      | 0.0111        | —            | 310                 |
| 3   | 0.0088              | 0.0133                 | 0.0097        | —            | 345                 |
| 4   | 0.0083              | 0.0116                 | 0.0088        | —            | 372                 |
| 5   | 0.0082              | 0.0091                 | 0.0089        | —            | 392                 |
| 6   | $\infty$            | 0.0088                 | 0.0086        | —            | 411                 |
| 7   | $\infty$            | 0.0088                 | $\infty$      | —            | 435                 |
| 8   | $\infty$            | $\infty$               | $\infty$      | —            | —                   |

Note:  $\infty$  means the simulation is unstable.

**Fig. 7.** Indicative computation times of the original (MOC + Zielke), the optimized (MOC + Trikha), and the new (FDTD + ADE) numerical methods as a function of the observation time for the Holmboe and Rouleau (1967) test case. These are the same parameters as in Table 3, except  $\Delta t = 61.5 \mu\text{s}$ .

## Discussion

The ADE method, as well as the recursive methods presented by Trikha (1975) and Suzuki et al. (1991), allow the numerical computation of the unsteady friction term with only  $(N + 2)$  variables to be stored at each step. Given the nowadays computational means, one approach could be to adopt a very accurate weighting function with  $N > 10$  systematically. This would imply the  $n_i$  coefficients to be larger than  $n_{10}$ . Unfortunately, this approach is limited by the stability of the numerical schemes, as presented in Table 4 for  $N > 6$ . A stability condition comparable to the CFL condition [Eq. (19)] is associated with the parameters  $n_i$ . As a rule of thumb, the parameters  $n_i \Delta t / \theta$  must not be too large. More specifically, the time step must satisfy the stability condition  $n_i \Delta t / \theta \leq \epsilon$ , in particular  $n_N \Delta t / \theta \leq \epsilon$ , where  $\epsilon$  is a threshold that depends on the time-integration scheme. For instance, this threshold is equal to 2.78 for the standard fourth-order Runge-Kutta algorithm and to 4.07 for RK46-L. This condition originates from the ADE formulation. Thus, ignoring the coupling term  $\partial V / \partial t$  for simplification, the ADE equations in Eq. (16) have the form  $dy/dt = \lambda y$ , with  $\lambda = -n_i / \theta$ . For the numerical solution to be bounded,  $\lambda \Delta t$  has to be located in the stability region of the

time-integration scheme (e.g., LeVeque 2007). Consequently, if  $n_i \Delta t / \theta$  is too large, the simulations are expected to be unstable. A detailed stability analysis of the whole system of partial differential equations in Eq. (17) is performed in the Appendix. As  $n_N$  increases approximately exponentially with  $N$ , this stability condition restricts the possible values of  $N$ . Thus, with the simulation parameters indicated in Table 3, the simulation becomes unstable for  $N > 6$ . The use of higher values of  $N$  is possible but at a price of a very small time step and, therefore, of an increased computational cost.

## Further Works

When presenting the Bode plot of  $W_{app}$  (Fig. 3), the reader may have noticed that the exact weighting function is very similar to the frequency response function of a fractional system of order  $1/2$ . Thus, searching for a very accurate approximation into an exponential sum with only a few terms is vain—precisely because it attempts to fit with first-order systems. One alternative to the numerical methods presented previously could be the use of numerical schemes adapted to fractional systems, such as the diffusive representation method (Monteghetti et al. 2016) or finite-difference method based on the Grünwald-Letnikov approximation of fractional derivatives (Scherer et al. 2011). Another alternative could be the convolution quadrature method (Lubich 1988). It is based on the insertion of the Laplace transform of the weighting function in the convolution and would therefore prevent the approximation of the weighting function by an exponential sum.

## Conclusions

Two improvements to the WFB method have been presented. First, a new method for the approximation of the unsteady friction weighting function into an exponential series has been derived. It is based on a rational approximation similar to a system identification procedure in the Laplace domain. Among the existing approximate functions, the resulting exponential series offers the best trade-off between validity and accuracy for a number of terms  $N \in [5, 9]$ . Accordingly, the new approximate functions in this range extend the validity, accuracy, and efficiency of the WFB method. Second, the ADE method has been introduced to compute the unsteady friction term. It consists of replacing the evaluation of the convolution with the time integration of a set of additional differential equations. Therefore, the ADE method no longer requires the assumption of a constant acceleration between two consecutive time steps. It is therefore appropriate for high-order numerical schemes. An experimental test case has been simulated thanks to the derived numerical methods. Simulation results were found to be very similar to the measurements. Finally, the numerical stability has been studied in detail for a Runge-Kutta time-integration scheme. A condition that restricts the maximum value of the exponential series coefficients has been derived from this analysis. Given a reasonably small time step, a limit on the number of terms arises for the simulation to be stable. Because the new approximation method of the weighting function can be very accurate if a high number of terms is set, the numerical stability can then be considered as a new limit on the application of the WFB method.

## Appendix. Stability Analysis

The rule of thumb that  $n_i \Delta t / \theta$  should be smaller than a given threshold is described by performing a stability analysis of Eq. (17).

With this aim, a pipe of infinite length is considered, and a spatial Fourier transform, using the convention  $e^{jkx}$ , is applied to Eq. (17)

$$\begin{aligned} \frac{d\tilde{H}}{dt} &= -\frac{a^2}{g} jk^* \tilde{V} \\ \frac{d\tilde{V}}{dt} &= -gjk^* \tilde{H} - \frac{4}{\theta} \left( 2\tilde{V} + \sum_{i=1}^N m_i \tilde{I}_i \right) \\ \frac{d\tilde{I}_i}{dt} &= -\frac{n_i}{\theta} \tilde{I}_i - \frac{d\tilde{V}}{dt} \end{aligned} \quad (22)$$

where  $\tilde{y}$  = spatial Fourier transform of  $y$ ; and the parameter  $k^*$ , called the effective wavenumber, is obtained from the Fourier transform of Eq. (18) as follows

$$k^* = \frac{2}{\Delta x} \sum_{i=1}^n c_i \sin(ik\Delta x) \quad (23)$$

Its deviation from the exact wavenumber  $k$  represents the numerical error introduced by discretizing the first derivative  $\partial/\partial x$  by a finite-difference scheme. Eq. (22) can then be recast in the form  $d\tilde{y}/dt = \mathbf{A}\tilde{y}$ , with the unknown vector  $\tilde{y} = [\tilde{H} \ \tilde{V} \ \tilde{I}_i]^T$ , and the matrix  $\mathbf{A}$  is given as follows

$$\mathbf{A} = \begin{pmatrix} 0 & -\frac{a^2}{g} jk^* & 0 & \cdots & 0 \\ -jgk^* & -\frac{8}{\theta} & -\frac{4m_1}{\theta} & \cdots & -\frac{4m_N}{\theta} \\ jgk^* & \frac{8}{\theta} & \frac{4m_1 - n_1}{\theta} & \cdots & \frac{4m_N}{\theta} \\ \vdots & \vdots & \vdots & \ddots & \vdots \\ jgk^* & \frac{8}{\theta} & \frac{4m_1}{\theta} & \cdots & \frac{4m_N - n_N}{\theta} \end{pmatrix} \quad (24)$$

The stability region of a time-integration scheme is defined as the set of points in the complex  $\lambda\Delta t$ -plane in which the numerical solution of the ordinary differential equation  $d\tilde{y}/dt = \lambda\tilde{y}$  is bounded. For a system of equations such as the discrete system given by Eq. (17), a necessary condition for the numerical solution to be stable is that all the eigenvalues  $\lambda$  of the matrix  $\mathbf{A}$  are located in the stability region (LeVeque 2007).

These eigenvalues can be determined analytically for  $N = 1$  and  $k = 0$ , for which the matrix  $\mathbf{A}$  simplifies to

$$\mathbf{A} = \begin{pmatrix} 0 & 0 & 0 \\ 0 & -\frac{8}{\theta} & -\frac{4m}{\theta} \\ 0 & \frac{8}{\theta} & \frac{4m - n}{\theta} \end{pmatrix} \quad (25)$$

where the first eigenvalue is  $\lambda = 0$ . The two other ones, obtained from the characteristic polynomial of  $\mathbf{A}$ , are given

$$\lambda_{\pm} = \frac{4m - n - 8 \pm \sqrt{\Delta}}{2\theta} \quad (26)$$

with the following discriminant

$$\Delta = n^2 \left[ 1 - \frac{16 + 8m}{n} + \frac{16m^2 - 64m + 64}{n^2} \right] \quad (27)$$

From Tables 1 and 2, it is seen that the coefficients  $n_i$  are large and also larger than the corresponding  $m_i$ . Thus, simplifying

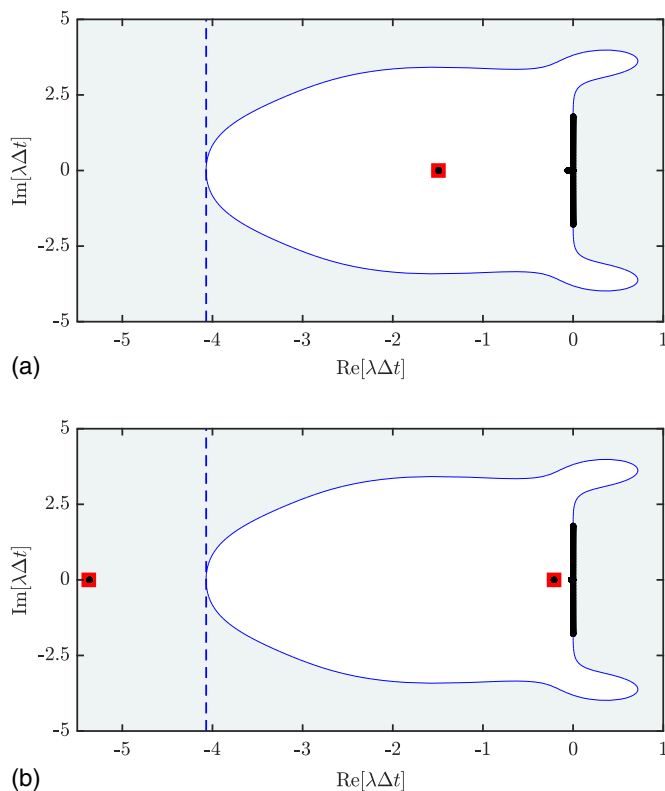


**Fig. 8.** Eigenvalues  $\lambda$  of the matrix  $\mathbf{A}$  in the complex  $\lambda\Delta t$ -plane for (a)  $N = 6$ ; and (b)  $N = 7$ . The stability region of RK46-L is indicated by the unshaded region, and the threshold is indicated by the dashed line.

Eq. (26) for  $n \gg m$  and  $n \gg 1$ , it can be shown that  $\lambda_+ \approx -8/\theta$ , while  $\lambda_- \approx -n/\theta$ . Therefore, for the simulation to be stable,  $-n/\theta$  should be in the stability region of the time-integration scheme.

For the case considered previously in the section “Simulation Test Case,” the eigenvalues  $\lambda$  of  $\mathbf{A}$  are determined numerically with the MATLAB version 2020a function eig.m version R2006a. Using the parameters indicated in Table 3, the eigenvalues scaled by  $\Delta t$  and computed for  $0 \leq k\Delta x \leq \pi$  and for  $N = 6$  and 7 are plotted in the  $\lambda\Delta t$ -plane in Fig. 8.

The stability region of the Runge-Kutta scheme RK46-L is also indicated and corresponds to the unshaded region. Thus, if an eigenvalue is located outside this region, the discrete system of equations is expected to be unstable. For  $N = 6$ , all the eigenvalues are enclosed within the stability region. Eigenvalues are mostly located along the imaginary axis, which corresponds to wave solutions. However, some eigenvalues are located along the real axis close to  $\lambda\Delta t = -1.5$ , which is approximately equal to  $-n_6\Delta t/\theta$ . For  $N = 7$ , the locations of the eigenvalues can be identified in the same manner. In particular, some eigenvalues are located close to  $\lambda\Delta t = -n_7\Delta t/\theta$  and  $-n_6\Delta t/\theta$ . In this case, as  $n_7\Delta t/\theta = 5.39$  is larger than the maximal admissible value for this Runge-Kutta algorithm equal to 4.07, a group of eigenvalues is located outside the stability region. It is therefore expected that the simulation for  $N = 6$  is stable, while it is unstable for  $N = 7$ , which is actually observed.

To sum up, it has been shown that some eigenvalues of the matrix  $\mathbf{A}$  are close to  $-n_i/\theta$ . For these eigenvalues to be in the stability region, and, hence, for the solution to be stable, the condition  $n_i\Delta t/\theta \leq \epsilon$ , introduced previously in the “Discussion,” must be satisfied.

## Data Availability Statement

All data, models, or code that support the findings of this study are available from the corresponding author upon reasonable request.

## Acknowledgments

This work was supported by the LabEx Centre Lyonnais d’Acoustique of Université de Lyon, operated by the French National Research Agency (ANR-10-LABX-0060/ANR-11-IDEX-0007). This work is part of the project ESSENCYELE (*moteur ESSENCE injection directe hYbride Electrique abordable*), financed by the French Agency for Environment and Energy Management (ADEME).

## Notation

The following symbols are used in this paper:

- $a$  = wave speed (m/s);
- CFL = Courant-Freidrichs-Lewis number;
- $c_k$  = coefficients of finite-difference scheme;
- $E_W$  = approximation error;
- $g$  = gravitational acceleration (m/s<sup>2</sup>);
- $H$  = piezometric head (m);
- $h$  = friction term;
- $I_i$  = additional variables for ADE method;
- $i, j, n$  = integers;
- $J_i$  = Bessel function of first kind and order  $i$ ;
- $\mathcal{J}_i$  =  $i$ th modified quotient of Bessel functions;
- $j$  = complex number;
- $k$  = integer or wavenumber (m<sup>-1</sup>);
- $k^*$  = effective wavenumber (m<sup>-1</sup>);
- $m_i, n_i$  = coefficients of  $W_{\text{app}}$ ;
- $N$  = number of terms of  $W_{\text{app}}$ ;
- $N_t$  = number of time steps;
- $N_x$  = number of cells;
- $R$  = pipe inner radius (m);
- $s$  = complex angular frequency (s<sup>-1</sup>);
- $s'$  = dimensionless complex angular frequency;
- $t$  = time (s);
- $V$  = flow velocity (m/s);
- $W$  = weighting function;
- $W_{\text{app}}$  = approximative weighting function;
- $x$  = distance (m);
- $\alpha_i, \beta_i$  = coefficients of Zielke’s weighting function;
- $\epsilon$  = numerical stability threshold;
- $\Delta t$  = time step (s);
- $\Delta x$  = mesh size (m);
- $\theta$  = characteristic time of viscosity (s);
- $\lambda$  = wavelength (m) or eigenvalue (s<sup>-1</sup>);
- $\nu$  = kinematic viscosity (m<sup>2</sup>/s);
- $\rho$  = density (kg/m<sup>3</sup>);
- $\tau$  = dimensionless time; and
- $\tau_0$  = wall shear stress (Pa).

## References

- Berland, J., C. Bogey, and C. Bailly. 2006. “Low-dissipation and low-dispersion fourth-order Runge-Kutta algorithm.” *Comput. Fluids* 35 (10): 1459–1463. <https://doi.org/10.1016/j.compfluid.2005.04.003>.

- Berland, J., C. Bogey, O. Marsden, and C. Bailly. 2007. "High-order, low dispersive and low dissipative explicit schemes for multiple-scale and boundary problems." *J. Comput. Phys.* 224 (2): 637–662. <https://doi.org/10.1016/j.jcp.2006.10.017>.
- Bogey, C., and C. Bailly. 2004. "A family of low dispersive and low dissipative explicit schemes for flow and noise computations." *J. Comput. Phys.* 194 (1): 194–214. <https://doi.org/10.1016/j.jcp.2003.09.003>.
- Bogey, C., N. de Cacqueray, and C. Bailly. 2009. "A shock-capturing methodology based on adaptative spatial filtering for high-order non-linear computations." *J. Comput. Phys.* 228 (5): 1447–1465. <https://doi.org/10.1016/j.jcp.2008.10.042>.
- Brunone, B., M. Ferrante, and M. Cacciamani. 2004. "Decay of pressure and energy dissipation in laminar transient flow." *J. Fluids Eng.* 126 (6): 928–934. <https://doi.org/10.1115/1.1839926>.
- Brunone, B., U. M. Golia, and M. Greco. 1995. "Effects of two-dimensionality on pipe transients modeling." *J. Hydraul. Eng.* 121 (12): 906–912. [https://doi.org/10.1061/\(ASCE\)0733-9429\(1995\)121:12\(906\)](https://doi.org/10.1061/(ASCE)0733-9429(1995)121:12(906)).
- Chaudhry, M. H. 2014. *Applied hydraulic transients*. New York: Springer.
- Deschrijver, D., M. M. T. Dhaene, and D. D. Zutter. 2008. "Macromodeling of multiport systems using a fast implementation of the vector fitting method." *IEEE Microwave Wireless Compon. Lett.* 18 (6): 383–385. <https://doi.org/10.1109/LMWC.2008.922585>.
- Gustavsen, B., and A. Semylen. 1999. "Rational approximation of frequency domain responses by vector fitting." *IEEE Trans. Power Delivery* 14 (3): 1052–1061. <https://doi.org/10.1109/61.772353>.
- Gustavsen, B., and A. Semylen. 2006. "Improving the pole relocating properties of vector fitting." *IEEE Trans. Power Delivery* 21 (3): 1587–1592. <https://doi.org/10.1109/TPWRD.2005.860281>.
- Holmboe, E. L., and W. T. Rouleau. 1967. "The effect of viscous shear on transients in liquid lines." *J. Basic Eng.* 89 (1): 174–180. <https://doi.org/10.1115/1.3609549>.
- Jiang, D., S.-J. Li, P. Yang, and T.-Y. Zhao. 2015. "Frequency-dependent friction in pipelines." *Chin. Phys. B* 24 (3): 034701. <https://doi.org/10.1088/1674-1056/24/3/034701>.
- Kagawa, T., I. Lee, A. Kitagawa, and T. Takenaka. 1983. "High speed and accurate computing method of frequency-dependent friction in laminar pipe flow for characteristics method." [In Japanese.] *Trans. Jpn. Soc. Mech. Eng. Ser. A* 49 (447): 2638–2644. <https://doi.org/10.1299/kikaib.49.2638>.
- LeVeque, R. J. 2007. Vol. 98 of *Finite difference methods for ordinary and partial differential equations: Steady-state and time dependent problems*. Philadelphia: Society for Industrial and Applied Mathematics.
- Lubich, C. 1988. "Convolution quadrature and discretized operational calculus." *Numer. Math.* 52 (2): 129–145. <https://doi.org/10.1007/BF01398686>.
- Monteghetti, F., D. Matignon, E. Piot, and L. Pascal. 2016. "Design of broadband time-domain impedance boundary conditions using the oscillatory-diffusive representation of acoustical models." *J. Acoust. Soc. Am.* 140 (3): 1663–1674. <https://doi.org/10.1121/1.4962277>.
- Scherer, R., S. L. Kalla, Y. Tang, and J. Huang. 2011. "The Grünwald–Letnikov method for fractional differential equations." *Comput. Math. Appl.* 62 (3): 902–917.
- Schohl, G. A. 1993. "Improved approximate method for simulating frequency-dependent friction in transient laminar flow." *J. Fluids Eng.* 115 (3): 420–424. <https://doi.org/10.1115/1.2910155>.
- Suzuki, K., T. Taketomi, and S. Sato. 1991. "Improving Zielke's method of simulating frequency-dependent friction in laminar liquid pipe flow." *J. Fluids Eng.* 113 (4): 569–573. <https://doi.org/10.1115/1.2926516>.
- Taylor, S. E. M., D. N. Johnston, and D. K. Longmore. 1997. "Modelling of transient flow in hydraulic pipelines." *Proc. Inst. Mech. Eng., Part I: J. Syst. Control Eng.* 211 (6): 447–456.
- Trikha, A. K. 1975. "An efficient method for simulating frequency-dependent friction in transient liquid flow." *J. Fluids Eng.* 97 (1): 97–105. <https://doi.org/10.1115/1.3447224>.
- Troian, R., D. Dagna, C. Bailly, and M.-A. Galland. 2017. "Broadband liner impedance education for multimodal acoustic propagation in the presence of a mean flow." *J. Sound Vib.* 392 (Mar): 200–216. <https://doi.org/10.1016/j.jsv.2016.10.014>.
- Urbanowicz, K. 2018. "Fast and accurate modelling of frictional transient pipe flow." *J. Appl. Math. Mech.* 98 (5): 802–823. <https://doi.org/10.1002/zamm.201600246>.
- Vardy, A. E., and J. Brown. 2004. "Efficient approximation of unsteady friction weighting functions." *J. Hydraul. Eng.* 130 (11): 1097–1107. [https://doi.org/10.1061/\(ASCE\)0733-9429\(2004\)130:11\(1097\)](https://doi.org/10.1061/(ASCE)0733-9429(2004)130:11(1097)).
- Vardy, A. E., and K.-L. Hwang. 1991. "A characteristics model of transient friction in pipes." *J. Hydraul. Res.* 29 (5): 669–684.
- Vítkovský, J., M. Stephens, A. Bergant, M. Lambert, and A. Simpson. 2004. "Efficient and accurate calculation of Zielke and Vardy-Brown unsteady friction in pipe transients." In Vol. 2 of *Proc., 9th Int. Conf. on Pressure Surges*, 405–419. Chester, UK: BHR Group.
- Vítkovský, J., M. Stephens, A. Bergant, A. Simpson, and M. Lambert. 2006. "Numerical error in weighting function-based unsteady friction models for pipe transients." *J. Hydraul. Eng.* 132 (7): 709–721. [https://doi.org/10.1061/\(ASCE\)0733-9429\(2006\)132:7\(709\)](https://doi.org/10.1061/(ASCE)0733-9429(2006)132:7(709)).
- Zielke, W. 1968. "Frequency-dependent friction in transient pipe flow." *J. Basic Eng.* 90 (1): 109–115. <https://doi.org/10.1115/1.3605049>.